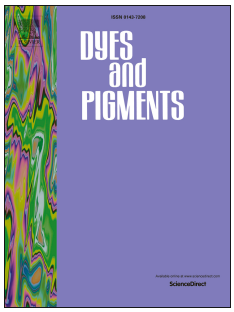

Functionalized carbon dots of thiazole derivatives based on inner filter effect for tetracyclines detection

Fanyong Yan, Zhonghui Sun, Jiping Pang, Yingxia Jiang, Wenxuan Zheng

PII: S0143-7208(20)31370-X

DOI: https://doi.org/10.1016/j.dyepig.2020.108673

Reference: DYPI 108673

To appear in: *Dyes and Pigments*

Received Date: 26 April 2020

Revised Date: 16 June 2020

Accepted Date: 26 June 2020

Please cite this article as: Yan F, Sun Z, Pang J, Jiang Y, Zheng W, Functionalized carbon dots of thiazole derivatives based on inner filter effect for tetracyclines detection, *Dyes and Pigments*, https://doi.org/10.1016/j.dyepig.2020.108673.

Declaration of interests

☑The authors declare that they have no known competing financial interests or personal relationships that could have appeared to influence the work reported in this paper.

☐The authors declare the following financial interests/personal relationships which may be considered as potential competing interests:

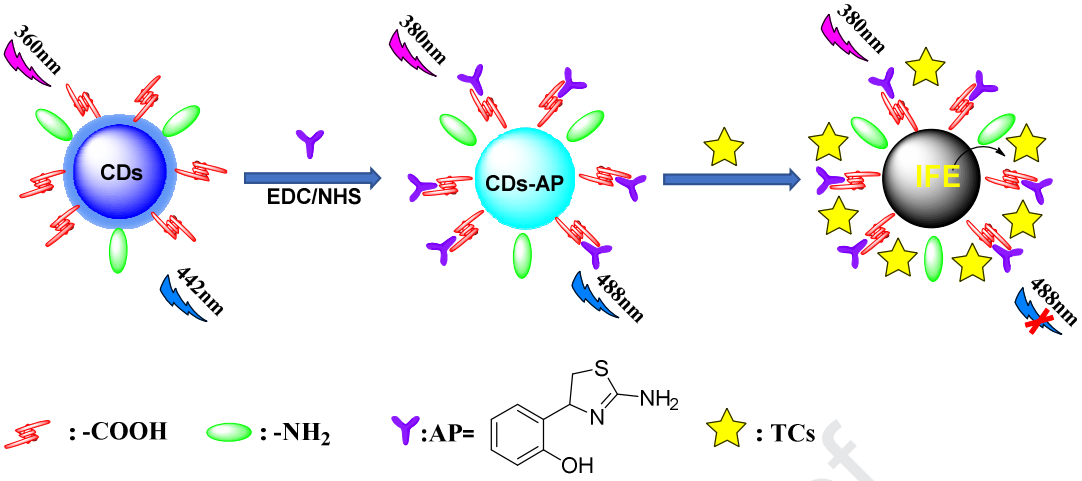

The schematic illustration of thiazole derivative-functionalized carbon dots (CDs-AP) for the detection of tetracyclines (TCs)

Functionalized carbon dots of thiazole derivatives based on inner filter effect for tetracyclines detection

Fanyong Yan[1]*, Zhonghui Sun[1], Jiping Pang[2]*, Yingxia Jiang[1], Wenxuan Zheng[1]

1. State Key Laboratory of Separation Membranes and Membrane Processes/National Center for International Joint Research on Separation Membranes, School of Chemistry and Chemical Engineering, Tiangong University, Tianjin 300387, PR China
2. Tianjin Zhongxin Pharmaceutical Group Co., Ltd. Zhongxin Pharmaceutical Factory

*Corresponding author. Tel: +86 22 83955766. E-mail addresses: yanfanyong@tiangong.edu.cn (Fanyong Yan);

Abstract

In this paper, we have developed a fluorescent probe based on thiazole derivative-functionalized carbon dots (CDs-AP) for the rapid, simple, and selective testing of commonly used antibiotics tetracyclines (TCs). Using citric acid (CA) and diethylenetriamine (DETA) as precursors, CDs rich in carboxyl groups were first synthesized, and then thiazole derivatives (AP) were covalently attached to the surface of CDs through an amidation coupling reaction. CDs-AP has high quantum yield (QY), excellent stability and good solubility. Response surface methodology (RSM) and the central composite design (CCD) were used to evaluate and optimize the operating parameters, including temperature, reaction time, and pH. Under the best operating conditions, CD-AP shows a good linear relationship for tetracycline (TET, an example for TCs), with a range of 0 – 18 μM and a detection limit of 0.7 nM. After detailed research, the inner filter effect (IFE) was proposed as the sensing mechanism. In addition, the probe has been successfully used for the determination of TET in milk samples and cell imaging for MDA-MB-231 cells.

Keywords:

Carbon dots; Functionalized; Inner filter effect; Tetracyclines detection; Response surface methodology; Cellular imaging

1. Introduction

TCs is a broad-spectrum antibacterial drug that can resist infections such as Gram-positive and negative bacteria, rickettsia, mycoplasma, spirochaetes, and parasites [1-3]. Because of its advantages of low cost and oral administration, it has been widely used to treat human and animal infections. The presence of TCs in the environment may accumulate in foods such as meat and milk and cause antibiotic resistance. Therefore, the large amount of TCs may pose a threat to human and animal health, such as the common tetracycline teeth. Common methods for the detection of tetracycline include high performance liquid chromatography (HPLC), electrochemical analysis and colorimetric method [4-6]. However, these methods have low sensitivity, tedious procedures, and time-consuming. The selection of appropriate probes for fluorescence detection has the advantages of a simple, high speed and sensitivity, so it has received widespread attention in the detection of antibiotics [7-9].

Compared with organic fluorescent dyes and traditional semiconductor quantum dots, the low cytotoxicity, high light stability, selectivity and sensitivity of inorganic nano carbon dots (CDs) make them more suitable for use in various fields [10-14]. The development of fluorescent probes based on CDs has attracted widespread attention and has been used for the detection of target analytes. Currently, many analytical techniques have been established based on the different quenching mechanisms between fluorophores and specific targets. The IFE is caused by the absorber (that is, the quencher) absorbing the excitation or emission light of the fluorophore, and the absorption band of the absorber should overlap the excitation or emission band of the fluorophore. And the quenching degree of fluorophore in IFE can be achieved by adjusting the concentration of absorbent [15, 16]. Compared with fluorescence resonance energy transfer (FRET) and photoinduced electron transfer (PET), in addition to the overlap between the absorption band of the absorber (acceptor) and the excitation or emission spectrum of the fluorophore (donor), IFE does not need to maintain a small distance between the quencher and the fluorophore, and no specific covalent connection is required between the fluorophore and the quencher [17, 18].

Here, we use CA as the carbon source and DETA as a nitrogen source, and firstly synthesized carboxyl-rich CDs that can be directly used for further surface modification by a one-step hydrothermal method. The prepared CDs and AP are covalently bonded to form CDs-AP. The successful synthesis of CDs-AP was confirmed by a series of characterization methods. Compared with CDs, the optimal excitation wavelength of CDs-AP changed from 360 nm to 380 nm, which overlaps with the absorption

spectrum of TCs. Therefore, TCs produced an effective IFE for CDs-AP, and the fluorescence of CDs-AP was quenched. Because different conditions will affect the sensitivity of CDs-AP to TET detection, the traditional method is cumbersome and does not consider the interaction between multiple factors. Therefore, by CCD and RSM to optimize the detection conditions such as pH, reaction time and temperature, the best operating conditions for detecting TET were obtained. In addition, CDs-AP has been further proven to be useful for TET detection of actual milk samples and cell imaging.

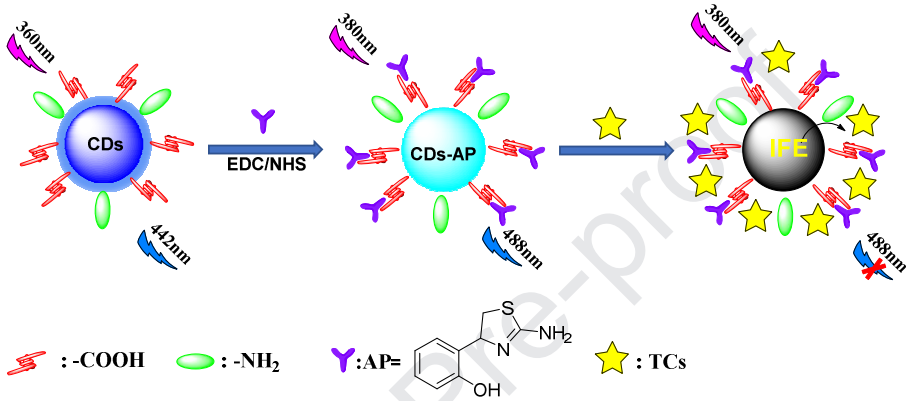

The schematic illustration of thiazole derivative-functionalized carbon dots (CDs-AP) for the detection of tetracyclines (TCs)

2. Experimental

2.1 Materials and apparatus

CA, o-hydroxyacetophenone, 1-ethyl-(3-dimethylaminopropyl) carbodiimide hydrochloride (EDC), and N-hydroxysuccinimide (NHS) were purchased from Shanghai Aladdin Biochemical Technology Co., Ltd. DETA, thiourea, glutathione (GSH), L-cysteine (Cys), homocysteine (Hcy), tyrosine (Tyr), glucose (Glu) and urea were purchased from Tianjin Damao Chemical Reagent Factory. TET, aureomycin hydrochloride (CTE), oxygen tetracycline (OXY), erythromycin (ERY), cefotaxime (CEF), ciprofloxacin (CIP), amoxicillin (AMX), and chloramphenicol (CHL) were purchased from Shanghai Maclean Biochemical Technology Co., Ltd. The milk was bought from a supermarket in Tianjin. All experimental drugs and reagents are of analytical grade, and experimental water is ultrapure water.

A fluorescence spectrum was made on a Hitachi F-4500 fluorescence spectrophotometer. The ultraviolet-visible (UV-vis) absorption spectrum was measured on a TU-1901 dual-beam UV-vis

spectrophotometer. Fourier Transform Infrared (FT-IR) spectra were collected on a VECTOR-22 FT-IR spectrophotometer; X-ray photoelectron spectroscopy (XPS) has been studied by an EDAX GENESIS spectrometer. Transmission electron microscopy (TEM) was performed on a JEOL-2010F type TEM. The fluorescence lifetime was recorded on a FLS1000 photoluminescence spectrometer.

2.2 Preparation of CDs

CDs are synthesized by a one-pot hydrothermal method. In short, CA (1.73 g, 7 mmol) and DETA (235 μL, 2.33 mmol) were dissolved in 30 mL of ultrapure water and sonicated for 10 min until completely dissolved. Then, the solution was transferred to a 50 mL polytetrafluoroethylene-lined reactor, and the temperature was raised to 180 °C for 3 h after preheating at 100 °C for 2 h. After cooling to room temperature, remove large insoluble particles through a 0.22 μm filter. The reaction mixture was then diluted with ultrapure water, and unreacted small molecule matter (MW = 3500 Da) was removed by dialysis for 48 h. Finally, the solvent was evaporated under reduced pressure to obtain 1.02 g yellow solid CDs.

2.3 Synthesis of AP

According to the previously reported method for the synthesis of 2-(2-amino-1,3-thiazol-4-yl)phenol (AP)[19]. As shown in Figure S1, thiourea (3.45 g, 0.045 mol), iodine (5.7 g, 0.045 mol), and o-hydroxyacetophenone (3.607 g, 0.03 mol) were dissolved in 40 mL of methanol was placed in a three-necked flask and heated and stirred at 90 °C for 30 min. After that, 5 mL of a 30% H_2O_2 solution was added dropwise to the front mixture, and the mixture was continuously heated for 4 h at 90 °C. When the reaction was complete, 30 mL of hot water was added to the mixture, and it was stirred at a constant temperature for 30 min, and the insoluble sulfur was filtered while hot. The mixed solution was then extracted with ether and the aqueous layers were combined. A certain amount of ammonia was added to the solution to adjust the pH to 8.0. The resulting insoluble white precipitate was filtered by suction and dried under vacuum. The resultant product was then recrystallized from an ethanol solution to obtain AP (1.66 g, 28.5 %, Melting Point: 139-140 °C).

2.4 Preparation of CDs-AP

CDs are conjugated to AP via an EDC/NHS reaction. Dissolve 0.4 g of CDs in 20 mL of absolute ethanol and adjust the pH to 6.8, then add 0.38 g (2 mmol) of EDC, stir for 30 min at ambient temperature to activate the carboxyl groups on the surface of the CDs, and then add 0.12 g (1 mmol) of NHS and 0.3 g of AP, protected from light and stirred for 48 h. After that, the solvent in the mixture was removed using a rotary evaporator, and the obtained mixed product was dissolved with a developing agent of CH_2Cl_2: CH_3OH = 20: 1, and separated by column chromatography. Finally, the solvent was removed by rotary evaporation and dried in vacuum at 60 °C for 6 h to obtain 0.08 g

CDs-AP. Take 0.05 g of product into a 25 mL volumetric flask and make up to volume with HEPES buffer (10 mM, pH 7.0) to obtain a 2 mg mL^{-1} CDs-AP stock solution.

2.5 Experimental design

In RSM, CCD is a commonly used experimental design for modeling and optimization. This method can find the best experimental conditions under the interaction of pH, reaction time and temperature [20-23]. In this experiment, we hope to find out the optimal conditions for detecting TET by the probe CDs-AP under the conditions of different pH, reaction time and temperature by CCD and RSM. In order to minimize the influence of non-control variables, 16 random experiments were choosed (Table 4-1). Then according to Fisher's statistical analysis, the results obtained are analyzed by analysis of variance. The relation between response (F/F_0) and detection variables is as follows:

$$\frac{F}{F_0} = +6.32 - 0.22X_1 + 0.4X_2 - 0.1X_3 + 0.032X_1X_2 + 0.14X_1X_3 + 0.17X_2X_3 - 1.48X_1^2 - 0.12X_2^2 \quad (1)$$

Where X_1, X_2 and X_3 are pH, reaction time and temperature, respectively.

2.6 Fluorescence detection of TET in HEPES buffer solution

TET was detected in HEPES buffer (10 mM, pH 7.0) at room temperature. First, 2 mg mL^{-1} of CDs-AP stock solution and 2×10^{-3} mol L^{-1} of TET and other analytes stock solution were prepared with HEPES buffer. Then add 100 μL of the CDs-AP stock solution and different volumes of TET stock solution to a 10 mL volumetric flask, and make up to volume with HEPES buffer. The test solution was shaken for 1 minute and then left at room temperature for 30 min. Finally, the fluorescence response was recorded using a fluorescence spectrometer. The excitation wavelength is 380 nm, and the excitation and emission slit widths are both 2.5 nm. Selective experiments were performed by adding 200 μL of other analytes and 100 μL of CDs-AP stock solution to 10 mL of HEPES buffer. The detection procedure was the same as above.

2.7 TET assay in real milk samples

The sample was processed according to the method in reference[24]: 5.0 mL of milk was accurately measured and placed in a 15 mL centrifuge tube, and then 2.0 mL of a 300 g / L trichloroacetic acid solution was added thereto and shaken sufficiently. After that, centrifuge at 5000 rpm for 10 minutes. Take the supernatant and let it stand for 5min, then filtered through a 0.45 μm aqueous cellulose acetate filter, and the filtrate was collected for later use. The detection process of TET in milk samples is: under the optimal conditions, take 100 μL of 2 mg mL^{-1} of CDs-AP mother liquor into a 10 mL volumetric flask, and then add a certain concentration of TET solution and the

20-fold diluted milk supernatant (0.5 mL), and make up to volume with HEPES buffer and shake up. After resting for 15 min, the relative fluorescence intensity of the solution was measured when the excitation wavelength was 380 nm.

2.8 Fluorescence imaging in MDA-MB-231 cells

The toxicity of CDs-AP on MDA-MB-231 cells was evaluated by MTT assay. The cells were added to RPMI 1640 medium containing 10 % fetal bovine serum and they were incubated at 37 °C with 5 % CO_2 for 24 h. Then, add different concentrations of CDs-AP (0 – 3 mg mL^{-1}) and incubate for 24 h. The cell viability was calculated according to this equation: cell viability (%) = absorbance of the experimental group/absorbance of the blank control group × 100 %.

Add 2 mg mL^{-1} of CDs-AP solution to the medium and incubate with MDA-MB-231 cells at 37 °C for 4 h, then add 18 μM TET and incubate for 30 min. The cells were washed 3 times with PBS buffer solution, and fluorescence imaging of the cells was obtained by laser scanning confocal microscope, in which the emission intensity of CDs-AP was recorded under 380 nm excitation.

3. Results and discussion

3.1 Characterization of CDs and CDs-AP

In order to prove the successful synthesis of CDs-AP, the morphology and size of CDs and CDs-AP were characterized by TEM. The TEM, HRTEM and particle size distribution histograms of CDs and CDs-AP are shown in Figure 1. In the TEM images, CDs and CDs-AP are almost uniform, monodisperse, and nearly spherical. HRTEM images show that the lattice spacing of both is 0.23nm. The particle size distribution histograms show that the average particle diameters of CDs and CDs-AP are 3.0 nm and 3.2 nm, respectively. The results showed that the morphology of CDs did not change significantly after AP functionalization, while the size of CDs increased slightly.

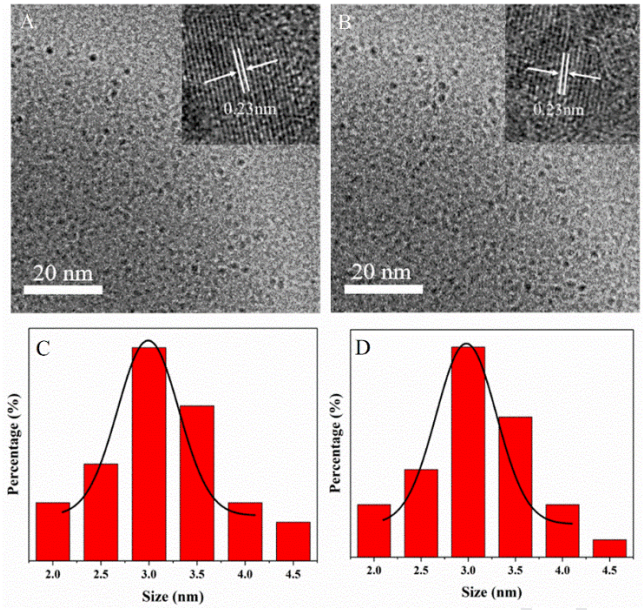

Figure 1 TEM images of CDs (A), CDs-AP (B), the inset is the corresponding HRTEM; Particle size distribution histogram of CDs (C), CDs-AP(D)

FTIR, XPS and Zeta potential results further confirmed the successful combination of CDs and AP. The -COOH on the surface of CDs is activated by EDC and NHS and reacts with the amino group on the AP, so that CDs are covalently connected to the AP through an amide bond. The FT-IR spectra of AP, CDs and CDs-AP are displayed in Figure 2 (A). The strong bands at 3100 cm^{-1}, 1650 cm^{-1}, and 675 cm^{-1} in the AP spectrum are attributed to the characteristic peaks of -NH_2, C=N, and C-S, respectively. The peaks at 3498 cm^{-1} and 1705 cm^{-1} in CDs are due to the stretching vibrations of O-H and C=O. After AP modification, the characteristic absorption band of C=O at 1705 cm^{-1} in CDs moved to 1650 cm^{-1}, and the C-S characteristic band appeared at 675 cm^{-1} [25]. These results indicate that there is an amidation reaction between CDs and AP. The XPS spectrum of CDs-AP in Figure 2 (B) shows the characteristic peak of S_{2p} at 163.4 eV, which can also confirm the successful synthesis of CDs-AP. After dividing the peak of S_{2p}, it was found that the characteristic absorption peaks of $S_{2p1/2}$ and $S_{2p3/2}$ corresponded to 163.0 and 164.1 eV, respectively. Figure 2 (D), (E), (F) and (G), (H), (I) are high-resolution XPS spectra of CDs and CDs-AP C_{1s}, N_{1s} and O_{1s}, respectively. In addition, zeta potential was used to further verify the generation of CDs-AP. As shown in Figure S2, due to the presence of many -COOH on the surface, the zeta potential of CDs is -14.51 mV. The amide bond formed by the modification of AP on the surface of CDs changed the Zeta potential of CDs-AP to -6.73 mV.

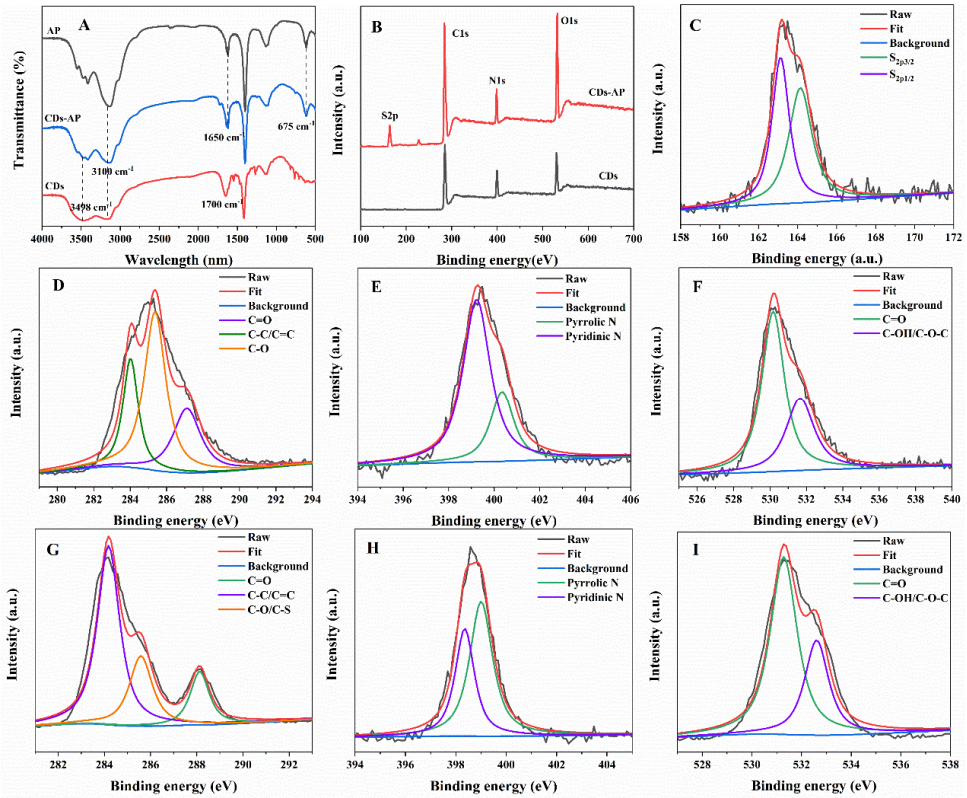

Fig 2 (A) FTIR spectra of CDs, AP and CDs-AP; (B) XPS spectra of CDs and CDs-AP; (C) S_{2p} spectra of CDs-AP; (D), (E), (F) and (G), (H), (I) are C_{1s}, N_{1s} and O_{1s} spectra of CDs and CDs-AP, respectively

In order to study the optical properties of CDs and CDs-AP, the fluorescence and UV-vis absorption spectroscopy were characterized. The UV-vis absorption spectra of CDs, AP, and CDs-AP are observed in Figure 3 (A). CDs has a typical absorption band at 350 nm, which is related to the n-π* transition of C=O. The absorption peaks of AP are observed at 215 and 230 nm, attributing to the π-π* transition of C=C and the n-π* transition of C=N, respectively [26]. After covalent coupling, a common characteristic peak of CDs and AP was observed in the UV-vis absorption of CDs-AP. Among them, the peak at 210 nm corresponds to the maximum absorption of AP at 215 nm, and the peak at 370 nm is due to the red shift caused by the n-π* transition of CDs at 350 nm, which also indicates that AP was successfully modified on the surface of CDs .

The fluorescence spectra of CDs as shown in Figure 3 (B). When the excitation wavelength is changed, the emission peaks of CDs show excitation-independent fluorescence characteristics. When the excitation wavelength is 360 nm, CDs have the strongest fluorescence emission at 442 nm. As displayed in Figure 3 (B), the fluorescence emission spectra of CDs-AP at an excitation wavelength from 330 nm to 430 nm. CDs-AP has the fluorescence characteristic that excitation determines the emission. When the excitation wavelength is 380 nm, the optimal fluorescence emission wavelength is 488 nm. Taking quinine sulfate as the reference, the fluorescence QYs of CDs and CDs-AP were 51.2 %

and 44.7 %, respectively. Figure 3 (D) shows the corresponding emission wavelengths of CDs and CDs-AP when the excitation wavelength is from 340 nm to 400 nm. The inset in Figure 3 (D) is a fluorescent image of CDs and CDs-AP dispersed in HEPES buffer under sunlight and ultraviolet light. CDs showed strong blue emission, and CD-AP showed blue-green fluorescence.

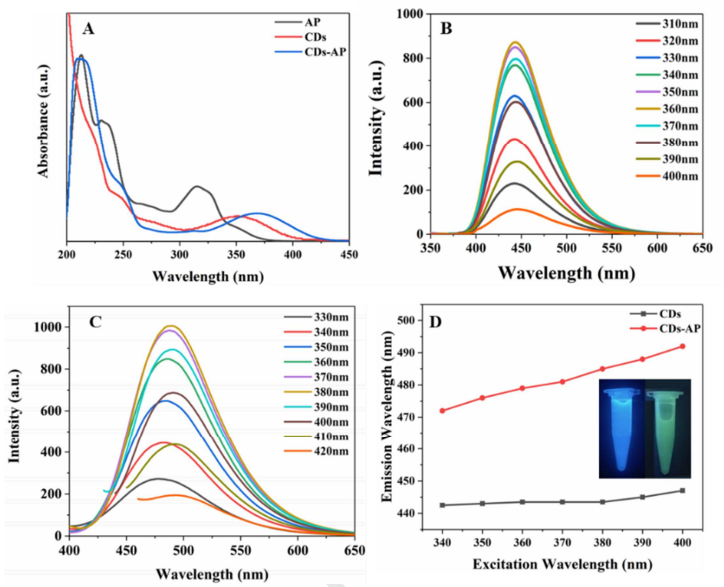

Fig. 3 (A) UV spectra of CDs, AP and CDs-AP; (B) Fluorescence emission spectra of CDs; (C) Fluorescence emission spectra of CDs-AP; (D) Line chart of CDs and CDs-AP emission wavelengths at different excitation wavelengths. Inset: fluorescence photography of CDs (left) and CDs-AP (right) under UV lamp

3.2 Optimization of detecting conditions

The optimal conditions of CDs-AP for TET detection were evaluated by CCD and RSM [133-134]. In this method, analysis of variance can find out the factors that have a significant impact on the actual analysis and their interactions. The P value in Table S2 is less than 0.05 and the F value is greater than 0.05, indicating a remarkable model correlation between the detection variables and F/F_0. In addition, the Conformance between the correlation coefficient R^2 = 0.9755 and the adjusted R^2 = 0.9676 can explain the huge correlation between the experimental data and the empirical model, which also shows that the model can effectively predict the response.

The relation between the predicted and real values of the model can be seen from Figure 4 (A). The real data are linearly distributed, which indicates that the model established in the experiment has enough consistency and stability with the actual data. The normal probability plot of the residuals is

shown in Figure 4 (B). The residuals in the figure fall approximately on a straight line, which indicates that the errors of this experiment are normally distributed. The relationship between the irregular residuals and the number of trials (Figure 4C) shows that the experimental model can correctly present the actual data. Therefore, the model is feasible for designing the detection conditions of the process.

Figure 5 shows the response to the fluorescence intensity of CDs-AP under the influence of one factor remaining constant and the other two factors. Among them, 1, 0.5, 0, -0.5, and -1 in turn represent the pH: 3, 5, 7, 9 and 11, the time is: 0, 5, 10, 15 and 20, and the temperature is 5, 15, 25, 35 and 45 ° C. The abscissa represents temperature, pH, and time, and the ordinate represents the difference between the fluorescence intensity of CDs-AP and the fluorescence intensity after adding TET under the corresponding conditions. Figure 5 (A) and (B) depict the effect of temperature on the response value. It can be analyzed from the figure that the quenching degree of CDs-AP increases first and then decreases with the increase of temperature, and 25 □ is the best detection temperature. The response surface affected by reaction time is shown in Figures 5 (B) and (C). When the reaction time was 10 min, the fluorescence response was the best, so 10 min is the optimal detection time. This shows that CDs-AP can respond quickly to TET. The effect of TET on the quenching degree of CDs-AP in the pH range of 3 – 11 as shown in Figures 5 (A) and (C). The optimal response pH is about 7.0. Therefore, when the temperature is 25 °C, the time is 10 min, and the pH is 7, the best detection conditions for the following experiments.

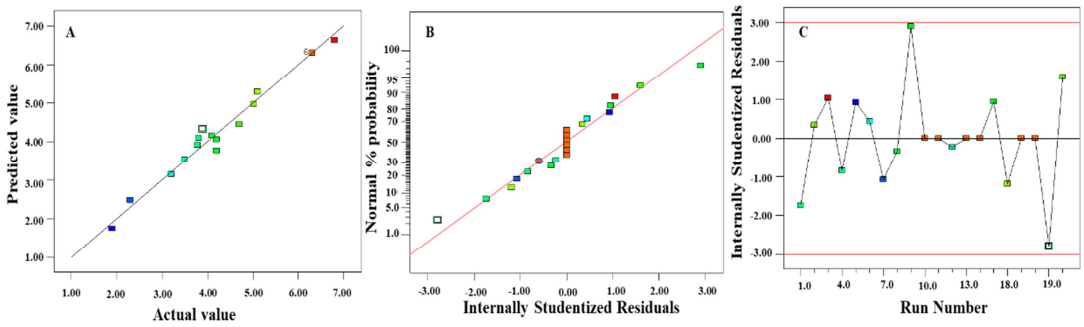

Fig 4 (A) Predicted vs. actual values plot (B) Normal probability plot of residuals (C) Run number vs. internally studentized residual plot

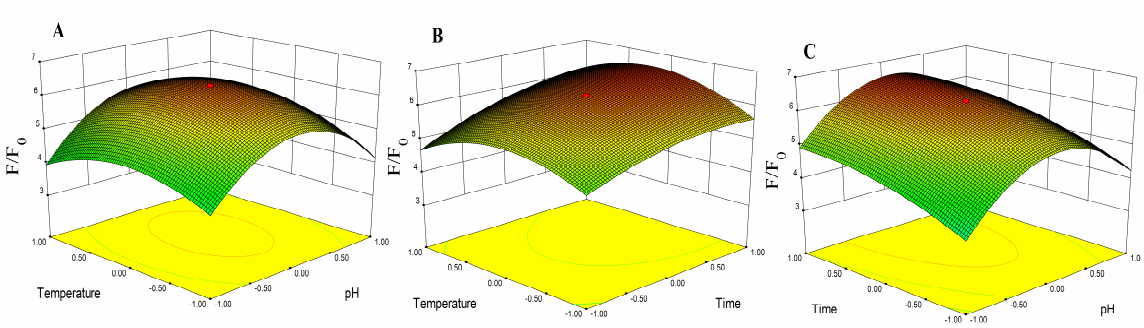

Fig 5 Response surfaces plot for CCD: (A) Temperature-pH (B) Temperature-Time (C) Time-pH

3.3 Fluorescence detection of CDs- AP to TET

In the optimum operating conditions, the fluorescence response of CDs-AP to TET was detected. The fluorescence intensity ratio (F/F_0) is used to reflect the fluorescence change before and after adding TET, where F_0 is the fluorescence intensity of pure CDs-AP solution, and F is the fluorescence intensity of CDs-AP solution after adding TET. As shown in Figure 6 (A), with the increase of TET concentration, the fluorescence intensity of CDs-AP under 380 nm excitation gradually decreases. There is a good linear relationship between F/F_0 and TET concentration in the range of 0 – 18 μM (inset in Figure 6A). The linear regression equation is F/F_0 = -0.0349[TET] +0.9638, and the correlation coefficient R^2 is 0.993. According to 3σ/k, the detection limit of TET for CDs-AP is 0.7 nM. Compared with other reported fluorescence sensors for detecting TET, CDs-AP displays better sensitivity, wider linear range and lower limit of detection for TET (Table 1).

In order to study the selectivity of CDs-AP for TET, we further examined the fluorescence response of di□erent kinds of antibiotics (including TET, CTE, OXY, ERY, CEF, CIP, AMX and CHL) and some coexisting potentially interfering substances (including Na^+, K^+, Ca^{2+}, Zn^{2+}, Fe^{2+}, Mg^{2+}, GSH, Cys, HCy, Tyr, Glu, urea) to CDs-AP. As shown in Figure 6 (B), the introduction of TET, CTE and OXY (all belong to TCs) caused a significant decrease in the fluorescence intensity of CDs-AP, and the fluorescence intensity of CDs-AP did not change after adding other substances of the same concentration. These results indicate that CDs-AP has a good specific fluorescent response to TCs.

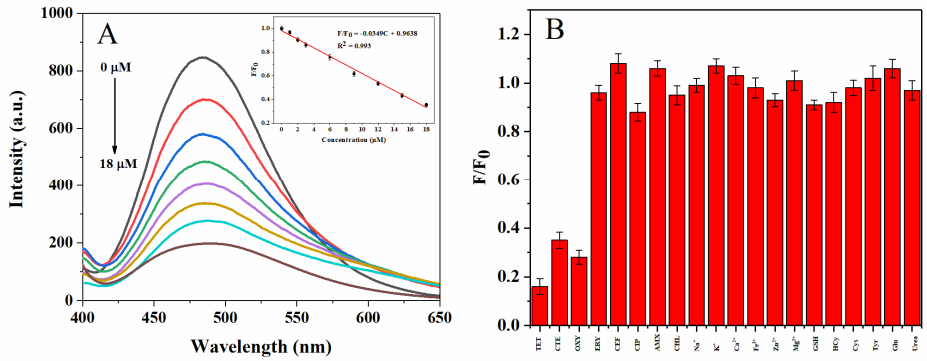

Fig 6 (A) The fluorescence spectra of CDs-AP in the presence of different concentration of TET. Inset: the linear relationship of F/F_0 and TET concentration (0 – 18μM); (B) The fluorescence response of CDs-AP in the presence of TET and other analytes. The concentration of all analytes was 20 μM.

Table 1. Comparison of the reported fluorescence probes with CDs-AP for TET detection

Probes	Detection range (μM)	Detection limit (nM)	References
HMIP@CDs	0.0225 – 0.45	6.96	[27]
g-C_3N_4-CdS	0.01 – 0.25	5.3	[28]
GQDs-Eu^{3+}	0 – 20	8.2	[29]
NIR-CDs	0.01 – 0.2	0.5	[30]
CDs	10 – 400	6000	[31]
Eu-MOF	0.05 – 160	17	[32]
MIPs@rCDs/bCDs@SiO_2	0 – 0.05	1.19	[33]
CDs-AP	0 – 18	0.7	This work

3.4 Detection mechanism of CDs- AP to TET

IFE usually occurs between the quencher and the fluorophore because the quencher absorbs the excitation or emission light of the fluorophore in the detection system. Effective IFE requires that the absorption band of the quencher overlaps with the excitation or emission band of the fluorophore [34].Therefore, choosing the right quencher and fluorophore is very important in IFE. As shown in Fig. 7 (A), TET has a broad absorption peak around 200 to 400 nm. However, the optimal excitation spectrum of the modified CDs-AP in the range of 300 to 425 nm can overlap with the absorption spectrum of TET in a large area. Therefore, TET can shield the excitation light of CDs-AP, resulting in the fluorescence quenching of CDs-AP.

In order to prove that the fluorescence quenching of CDs-AP by TET is through IFE, the time-resolved fluorescence spectra of CDs-AP and CDs-AP and TET system are shown in Figure 7 (B). In the absence of TET (black curve), the fluorescence lifetime of CDs-AP is about 11.96 ns (χ^2 = 1.117). In the presence of 20 μM TET (red curve), the fluorescence lifetime of CDs-AP is 11.48 ns (χ^2 = 1.097). The fluctuation of the two is less than 1 ns, thus excluding the mechanism of dynamic quenching and FRET. The almost unchanged fluorescence lifetime indicates that there is no interaction between CDs-AP and TET in the excited state, but is caused by simply absorbing the excitation light of CDs-AP [35]. Therefore, we can confirm that the mechanism for CDs-AP to detect TET is IFE.

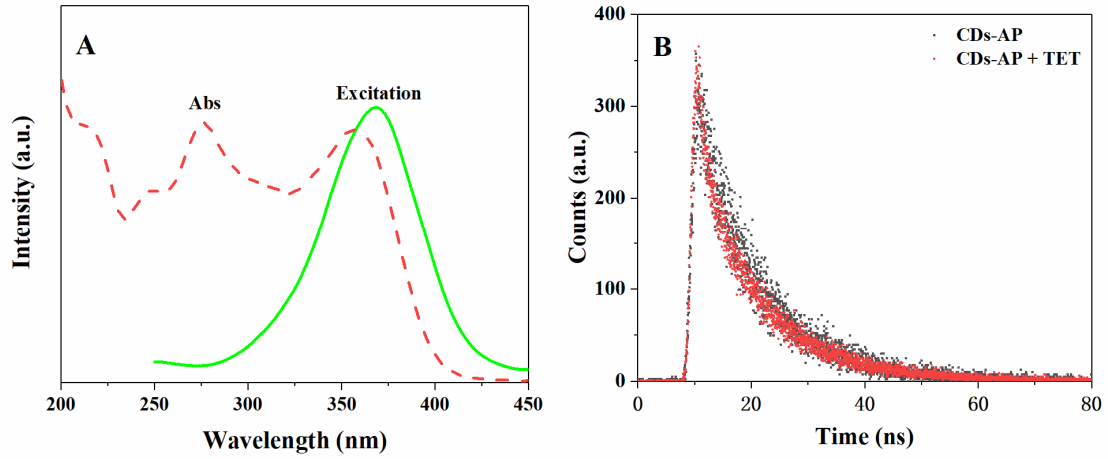

Fig 7 (A) The maximum excitation spectrum of CDs-AP and UV-vis absorption spectrum of TET. (B) The fluorescence decay curves of CDs-AP before and after adding TET (18μM)

3.5 Detection of TET in real milk samples

Since no TET was detected directly in the milk sample, which indicates that TET was qualified in the milk examined. Next, we performed fluorescence detection by adding different amounts of TET to milk samples. Table 2 shows the results of the experiment. The recoveries were in range of 98.5 to 104.0% with RSD ranging from 2.2% to 4.1%. This is acceptable for the quantitative analysis of TET in actual milk samples. Standard addition experiments of TET in milk samples show that CDs-AP has the potential to detect TET in actual samples.

Table 2. Analytical results of TET in spiked milk samples based on CDs-AP

Samples	Measured	Added	Found	Recovery	RSD*

	（μM）	（μM）	（μM）	（%）	(%, n=3)
1	ND*	2.00	1.97	98.5	2.2
2	ND*	4.00	4.16	104．0	4.1
3	ND*	6.00	6.09	101.5	2.4
4	ND*	8.00	7.98	99.8	3.2

ND*: not detect.

3.6 MDA-MB-231 cells imaging of CDs-AP

We used the MTT assay to study the toxicity of CDs-AP on MDA-MB-231 cells. As shown in Figure S3, when the concentration of CDs-AP reaches 3 mg mL^{-1}, the cell activity is still greater than 80 %, which indicates that CDs-AP has low toxicity to MDA-MB-231 cells. Due to the low toxicity and good biocompatibility of CDs-AP, we further conducted MDA-MB-231 cell imaging experiments. Figure 8C shows that after adding CDs-AP, MDA-MB-231 cells emit obvious blue-green fluorescence. After the addition of TET, the blue-green fluorescence is almost quenched (Figure 8D). This indicates that CDs-AP can enter the cell and exert its ability to respond to TET.

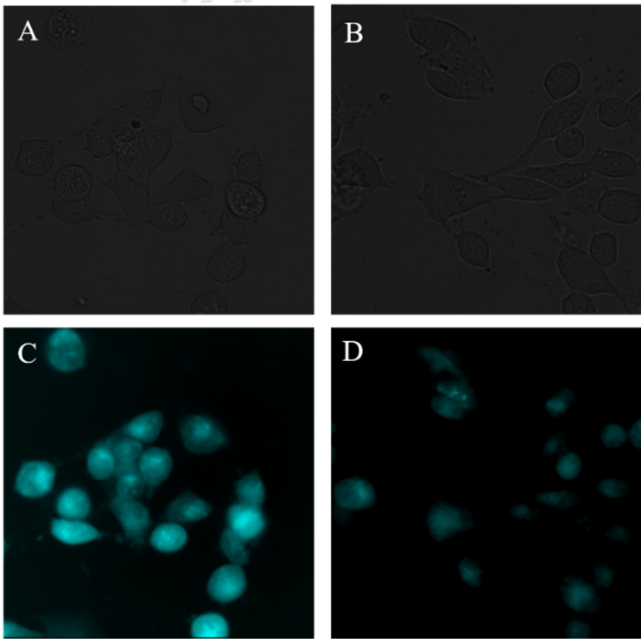

Fig 8 (A) Bright field confocal images of MDA-MB-231 cells incubated with 2 mg mL^{-1} CDs-AP; (B) Bright field confocal images of MDA-MB-231 cells incubated with 2 mg mL^{-1} CDs-AP and 18 μM TET ; (C) Black field confocal images of MDA-MB-231 cells incubated with 2 mg mL^{-1} CDs-AP; (D) Black field confocal images of MDA-MB-231 cells incubated with 2 mg mL^{-1} CDs-AP and 18 μM

TET

4. Conclusion

In this study, we first used CA and DETA as raw materials to prepare CDs rich in carboxyl groups on the surface by a simple solvothermal method. CDs-AP was then obtained by EDC-activated amidation coupling reaction. Their successful synthesis was characterized by TEM, XPS, etc., and the fluorescence and UV spectra of CDs and CDs-AP were studied. Compared with the original CDs, the excitation wavelength of CDs-AP can fully overlap the absorption spectrum of TCs, so that TCs quenches the fluorescence of CDs-AP through IFE. The central composite design (CCD) evaluates and optimizes the operating parameters during the inspection process. Under the optimal operating conditions, this highly stable fluorescent nanoprobe (CDs-AP) is used as a specific detection of TET. The detection limit is 0.7 nM in the linear range of TET concentrations from 0 – 18 μM. In addition, because the probe has high selectivity for TCs and low toxicity to MDA-MB-231 cells, it can be used for the detection of TET in actual milk samples and as a fluorescent imaging agent.

Acknowledgements

The work was supported by the National Natural Science Foundation of China (51678409, 51638011 and 51578375), Tianjin Research Program of Application Foundation and Advanced Technology (19JCYBJC19800, 18JCYBJC87500, 15ZCZDSF00880), State Key Laboratory of Separation Membranes and Membrane Processes (Z1-201507), and the Program for Innovative Research Team in University of Tianjin (TD13-5042)

References

[1] Taghdisi SM, Danesh NM, Ramezani M, Abnous K. A novel M-shape electrochemical aptasensor for ultrasensitive detection of tetracyclines. Biosensors and Bioelectronics. 2016;85:509-14.

[2] Tan H, Chen Y. Silver nanoparticle enhanced fluorescence of europium (III) for detection of tetracycline in milk. Sensors and Actuators B: Chemical. 2012;173:262-7.

[3] Wang J, Cheng R, Wang Y, Sun L, Chen L, Dai X, et al. Surface-imprinted fluorescence microspheres as ultrasensitive sensor for rapid and effective detection of tetracycline in real biological samples. Sensors and Actuators B: Chemical. 2018;263:533-42.

[4] Ma TY, Vickroy TW, Shien JH, Chou CC. Improved nonaqueous capillary electrophoresis for tetracyclines at subparts per billion level. Electrophoresis. 2012;33(11):1679-82.

[5] Peres GT, Rath S, Reyes FGR. A HPLC with fluorescence detection method for the determination of tetracyclines residues and evaluation of their stability in honey. Food Control. 2010;21(5):620-5.

[6] Jalalian SH, Karimabadi N, Ramezani M, Abnous K, Taghdisi SM. Electrochemical and optical aptamer-based sensors for detection of tetracyclines. Trends in Food Science & Technology. 2018;73:45-57.

[7] Ramezani M, Mohammad Danesh N, Lavaee P, Abnous K, Mohammad Taghdisi S. A novel colorimetric triple-helix molecular switch aptasensor for ultrasensitive detection of tetracycline. Biosensors and Bioelectronics. 2015;70:181-7.

[8] Liu X, Huang D, Lai C, Zeng G, Qin L, Zhang C, et al. Recent advances in sensors for tetracycline antibiotics and their applications. TrAC Trends in Analytical Chemistry. 2018;109:260-74.

[9] Shi W, Guo F, Han M, Yuan S, Guan W, Li H, et al. N,S co-doped carbon dots as a stable bio-imaging probe for detection of intracellular temperature and tetracycline. Journal of Materials Chemistry B. 2017;5(18):3293-9.

[10] Yan F, Jiang Y, Sun X, Wei J, Chen L, Zhang Y. Multicolor carbon dots with concentration-tunable fluorescence and solvent-affected aggregation states for white light-emitting diodes. Nano Research. 2019;13(1):52-60.

[11] Song E, Yu M, Wang Y, Hu W, Cheng D, Swihart MT, et al. Multi-color quantum dot-based fluorescence immunoassay array for simultaneous visual detection of multiple antibiotic residues in milk. Biosens Bioelectron. 2015;72:320-5.

[12] Yan F, Sun Z, Zhang H, Sun X, Jiang Y, Bai Z. The fluorescence mechanism of carbon dots, and methods for tuning their emission color: a review. Mikrochim Acta. 2019;186(8):583.

[13] Miao X, Qu D, Yang D, Nie B, Zhao Y, Fan H, et al. Synthesis of Carbon Dots with Multiple Color Emission by Controlled Graphitization and Surface Functionalization. Adv Mater. 2018;30(1).

[14] Zhi B, Cui Y, Wang S, Frank BP, Williams DN, Brown RP, et al. Malic Acid Carbon Dots: From Super-resolution Live-Cell Imaging to Highly Efficient Separation. ACS Nano. 2018;12(6):5741-52.

[15] Yan F, Zu F, Xu J, Zhou X, Bai Z, Ma C, et al. Fluorescent carbon dots for ratiometric detection of curcumin and ferric ion based on inner filter effect, cell imaging and PVDF membrane fouling research of iron flocculants in wastewater treatment. Sensors and Actuators B: Chemical. 2019;287:231-40.

[16] Zhang QQ, Chen BB, Zou HY, Li YF, Huang CZ. Inner filter with carbon quantum dots: A selective sensing platform for detection of hematin in human red cells. Biosens Bioelectron. 2018;100:148-54.

[17] Han L, Liu SG, Dong XZ, Liang JY, Li NB, Luo HQ. Construction of an effective ratiometric fluorescent sensing platform for specific and visual detection of mercury ions based on target-triggered the inhibition on inner filter effect. J Hazard Mater. 2019;376:170-7.

[18] Zu F, Yan F, Bai Z, Xu J, Wang Y, Huang Y, et al. The quenching of the fluorescence of carbon dots: A review on mechanisms and applications. Microchimica Acta. 2017;184(7):1899-914.
[19] Safari J, Abedi-Jazini Z, Zarnegar Z, Sadeghi M. Nanochitosan: A biopolymer catalytic system for the synthesis of 2-aminothiazoles. Catalysis Communications. 2016;77:108-12.
[20] Nemati F, Hosseini M, Zare-Dorabei R, Salehnia F, Ganjali MR. Fluorescent turn on sensing of Caffeine in food sample based on sulfur-doped carbon quantum dots and optimization of process parameters through response surface methodology. Sensors and Actuators B: Chemical. 2018;273:25-34.
[21] Ghafari S, Aziz HA, Isa MH, Zinatizadeh AA. Application of response surface methodology (RSM) to optimize coagulation-flocculation treatment of leachate using poly-aluminum chloride (PAC) and alum. J Hazard Mater. 2009;163(2-3):650-6.
[22] Calero J, Luna D, Luna C, Bautista FM, Romero AA, Posadillo A, et al. Optimization by response surface methodology of the reaction conditions in 1,3-selective transesterification of sunflower oil, by using CaO as heterogeneous catalyst. Molecular Catalysis. 2020;484:110804.
[23] Yan F, Jiang Y, Sun X, Ma T, Chen L, Chen L. 4-aminoantipyrine modified carbon dots and their analytical applications through response surface methodology. Spectrochimica Acta Part A: Molecular and Biomolecular Spectroscopy. 2020;227:117543.
[24] Li C, Zhu L, Yang W, He X, Zhao S, Zhang X, et al. Amino-Functionalized Al-MOF for Fluorescent Detection of Tetracyclines in Milk. J Agric Food Chem. 2019;67(4):1277-83.
[25] Chen S, Jia Y, Zou GY, Yu YL, Wang JH. A ratiometric fluorescent nanoprobe based on naphthalimide derivative-functionalized carbon dots for imaging lysosomal formaldehyde in HeLa cells. Nanoscale. 2019;11(13):6377-83.
[26] Liu H, Sun Y, Li Z, Yang J, Aryee AA, Qu L, et al. Lysosome-targeted carbon dots for ratiometric imaging of formaldehyde in living cells. Nanoscale. 2019;11(17):8458-63.
[27] Li H, Zhao L, Xu Y, Zhou T, Liu H, Huang N, et al. Single-hole hollow molecularly imprinted polymer embedded carbon dot for fast detection of tetracycline in honey. Talanta. 2018;185:542-9.
[28] Liu Y, Yan K, Zhang J. Graphitic Carbon Nitride Sensitized with CdS Quantum Dots for Visible-Light-Driven Photoelectrochemical Aptasensing of Tetracycline. ACS Applied Materials & Interfaces. 2016;8(42):28255-64.
[29] Li W, Yu X, Ma X, Xie L, Xia Z, Liu L, et al. Deguelin attenuates non-small cell lung cancer cell metastasis through inhibiting the CtsZ/FAK signaling pathway. Cellular Signalling. 2018;50:131-41.
[30] Qian S, Qiao L, Xu W, Jiang K, Wang Y, Lin H. An inner filter effect-based near-infrared probe for the ultrasensitive detection of tetracyclines and quinolones. Talanta. 2019;194:598-603.
[31] Yan Y, Liu JH, Li RS, Li YF, Huang CZ, Zhen SJ. Carbon dots synthesized at room temperature for detection of tetracycline hydrochloride. Anal Chim Acta. 2019;1063:144-51.
[32] Zhou Y, Yang Q, Zhang D, Gan N, Li Q, Cuan J. Detection and removal of antibiotic tetracycline in water with a highly stable luminescent MOF. Sensors and Actuators B: Chemical. 2018;262:137-43.
[33] Liu X, Wang T, Wang W, Zhou Z, Yan Y. A tailored molecular imprinting ratiometric fluorescent sensor based on red/blue carbon dots for ultrasensitive tetracycline detection. Journal of Industrial and Engineering Chemistry. 2019;72:100-6.
[34] Sun L, Zhou H, Huang D, Wang T, Gao P, Sun Y, et al. Fluorometric determination of antioxidant capacity in human plasma by using upconversion nanoparticles and an inner filter effect mechanism. Microchimica Acta. 2019;186(8):502.
[35] Hu Y, Gao Z. Yellow emissive Se,N-codoped carbon dots toward sensitive fluorescence assay of

crystal violet. J Hazard Mater. 2020;388:122073.

Highlights

1. Functionalized carbon dots of thiazole derivatives (CDs-AP) was used as the nanoprobe for the detection of tetracyclines (TCs) based on IFE.
2. Response Surface Methodology (RSM) based on the central composite design (CCD) was used to evaluate and optimize the operating parameters of tetracycline (TET, an example for TCs) detection.
3. CDs-AP was successfully applied for the detection of TET in milk samples and cell imaging for MDA-MB-231 cells.

Declaration of interests

☑The authors declare that they have no known competing financial interests or personal relationships that could have appeared to influence the work reported in this paper.

☐The authors declare the following financial interests/personal relationships which may be considered as potential competing interests: